

Constraints on Nuclear Saturation Properties from Terrestrial Experiments and Astrophysical Observations of Neutron Stars

SOONCHUL CHOI,^{1,2} TSUYOSHI MIYATSU ³, MYUNG-KI CHEOUN ¹, AND KOICHI SAITO ³

¹*Department of Physics and OMEG institute, Soongsil University, Seoul 156-743, Republic of Korea*

²*Center for Exotic Nuclear Studies, Institute for Basic Science, Daejeon 34126, Republic of Korea*

³*Department of Physics, Faculty of Science and Technology, Tokyo University of Science, Noda, 278-8510, Japan*

(Received; Revised; Accepted)

Submitted to

ABSTRACT

Taking into account the terrestrial experiments and the recent astrophysical observations of neutron stars and gravitational-wave signals, we impose restrictions on the equation of state (EoS) for isospin-asymmetric nuclear matter. Using the relativistic mean-field model with SU(3) flavor symmetry, we investigate the impacts of effective nucleon mass, nuclear incompressibility, and slope parameter of nuclear symmetry energy on the nuclear and neutron-star properties. It is found that the astrophysical information of massive neutron stars and tidal deformabilities as well as the nuclear experimental data plays an important role to restrict the EoS for neutron stars. Especially, the softness of the nuclear EoS due to the existence of hyperons in the core gives stringent constraints on those physical quantities. Furthermore, it is possible to put limits on the curvature parameter of nuclear symmetry energy by means of the nuclear and astrophysical calculations.

Keywords: dense matter — equation of state — stars: neutron

1. INTRODUCTION

Neutron stars are known to be the densest object in our universe. Since the first discovery of a pulsar (Hewish & Okoye 1965; Hewish et al. 1968), many theoretical studies regarding the understanding of neutron-star characteristics have been performed because the nature of neutron stars are broadly determined by the nuclear equation of state (EoS). At the present, neutron stars are believed to be cosmological laboratories for dense nuclear matter (Glendenning 1997; Lattimer & Prakash 2007). Conversely, the accurate data from astrophysical observations can enable us to select the appropriate EoSs for neutron stars, and thus it may be possible to figure out the properties of nuclear matter around and beyond the nuclear saturation density.

Thanks to the advanced technological development in science, some invaluable information due to astrophysical observations have been reported in the last decade. In particular, Shapiro delay measurements of a two-solar-mass neutron star have a great impact on the astrophysical and nuclear communities because it is very difficult to explain such massive neutron stars using the existing EoSs with exotic degrees of freedom, such as hyperons and/or kaon condensates (Glendenning & Moszkowski 1991; Schaffner-Bielich 2008). The binary millisecond pulsar, J1614-2230, has the mass of $1.97 \pm 0.04 M_{\odot}$ (Demorest et al. 2010), and it is recently updated to $1.908 \pm 0.016 M_{\odot}$ (Arzoumanian et al. 2018). The mass of PSR J0348+0432 is also estimated to be $2.01 \pm 0.04 M_{\odot}$ by a combination of radio timing and precise spectroscopy of the white dwarf companion (Antoniadis et al. 2013). Furthermore, an extremely massive millisecond pulsar, J0740+6620, has been found, and the mass is measured to be $2.14^{+0.10}_{-0.09} M_{\odot}$ (Cromartie et al. 2019).

In addition to the observations of massive neutron stars, a new type of observational data has been established by the gravitational wave (GW) from binary neutron star merger detected by the advanced LIGO and advanced Virgo observatories (Abbott et al. 2018, 2019). Because the GW signals of binary neutron-star inspirals can potentially yield robust information on the nuclear EoS, it is quite useful to consider the tidal deformability of a neutron star (Hinderer 2008; Hinderer et al. 2010). The dimensionless tidal deformability, Λ , is defined as $\Lambda = \frac{2}{3} k_2 \left(\frac{R}{M}\right)^5$, where k_2 is the second Love number, and M and R are, respectively, the mass and radius of a neutron star. Recently, many theoretical discussions have focused on the GW information and the tidal deformability (Annala et al. 2018; De et al. 2018; Most et al. 2018; Raithel et al. 2018; Lim & Holt 2018; Capano et al. 2020). They have reported that the tidal deformability of a canonical $1.4M_{\odot}$ neutron star, $\Lambda_{1.4}$, is highly sensitive to its radius, $R_{1.4}$, and the GW signals is of great use to give stringent constraints on the EoS for neutron-star matter (Chatziioannou et al. 2018; Kim et al. 2018; Malik et al. 2018; Radice et al. 2018; Tews et al. 2018, 2019; Zhao & Lattimer 2018; Lourenço et al. 2019; Wei et al. 2019).

From the viewpoint of nuclear physics, the nuclear symmetry energy, E_{sym} , is recognized to be a significant physical quantity to explain properties of finite nuclei and nuclear matter at low densities (Li et al. 2008; Danielewicz & Lee 2009). Although the characteristics of isospin-asymmetric nuclear matter in the density region beyond the nuclear saturation density are still under debate, much progress has been made in understanding the density dependence of E_{sym} based on various analyses of terrestrial experiments such as heavy-ion collisions (Li et al. 2014, 2019; Zhang et al. 2018; Xie & Li 2019; Miyatsu et al. 2020). Recently many calculations have focused on the correlation between E_{sym} and Λ to determine the EoSs for neutron-rich nuclear matter at supra-high densities (Fattoyev et al. 2018; Krastev & Li 2019; Raithel & Ozel 2019; Zhang & Li 2019).

In the present study, we restrict the nuclear EoSs based on the recent data of terrestrial experiments and astrophysical observations using the relativistic mean-field (RMF) model with a nonlinear potential (Walecka 1974; Boguta & Bodmer 1977; Serot & Walecka 1986; Todd-Rutel & Piekarewicz 2005a; Fattoyev et al. 2010). We take into account the semi-empirical data deduced from the realistic N - N interaction (Katayama & Saito 2013; Sammarruca et al. 2015) and the analyses of heavy-ion collisions (Tsang et al. 2012; Russotto et al. 2016) in the intermediate density region. Not only the tidal deformabilities (Abbott et al. 2018) but also the observed maximum masses of neutron stars (Antoniadis et al. 2013; Cromartie et al. 2019) are exploited to investigate the neutron-star properties. Moreover, hyperons as well as nucleons are explicitly included in the core of a neutron star within SU(3) flavor symmetry (Miyatsu et al. 2012, 2013a; Katayama et al. 2012; Weissenborn et al. 2012),

since the exotic degrees of freedom are known to soften the EoSs for neutron-star matter drastically and their effect is still an open question in the multi-messenger Era (Kumar et al. 2017; Li et al. 2018; Paschalidis et al. 2018; Zhou et al. 2018; Zhu et al. 2018; Li & Sedrakian 2019; Ribes et al. 2019; Sahoo et al. 2019; Fortin et al. 2020). At last, we present the calibrated EoSs for neutron stars and the preferable relations in nuclear saturation properties such as effective nucleon mass, nuclear incompressibility, and slope and curvature parameters of E_{sym} .

This paper is organized as follows. In Section 2, a brief review of the RMF model in SU(3) flavor symmetry is presented. Numerical results compatible for nuclear and neutron-star matter are presented with detailed discussions concerning the correlations among the important physical quantities in Section 3. Finally, we give a summary in Section 4.

2. THEORETICAL FRAMEWORK

For describing the properties of nuclear and neutron-star matter, we employ the usual Lagrangian density in RMF approximation (Walecka 1974; Serot & Walecka 1986). In addition, for the purpose of studying the impact of strangeness in the core of a neutron star, not only the σ , ω , and ρ mesons but also the strange mesons, namely the isoscalar, Lorentz scalar (σ^*) and vector (ϕ) mesons, are taken into account in SU(3) flavor symmetry (Miyatsu et al. 2012, 2013a; Katayama et al. 2012; Weissenborn et al. 2012). Since the charge neutrality and β equilibrium conditions are imposed in neutron-star calculations, leptons must be introduced as well. The Lagrangian density is thus chosen to be

$$\begin{aligned} \mathcal{L} = & \sum_B \bar{\psi}_B [i\gamma_\mu \partial^\mu - M_B^*(\sigma, \sigma^*) - g_{\omega B} \gamma_\mu \omega^\mu - g_{\phi B} \gamma_\mu \phi^\mu - g_{\rho B} \gamma_\mu \boldsymbol{\rho}^\mu \cdot \mathbf{I}_B] \psi_B \\ & + \frac{1}{2} (\partial_\mu \sigma \partial^\mu \sigma - m_\sigma^2 \sigma^2) + \frac{1}{2} (\partial_\mu \sigma^* \partial^\mu \sigma^* - m_{\sigma^*}^2 \sigma^{*2}) \\ & + \frac{1}{2} m_\omega^2 \omega_\mu \omega^\mu - \frac{1}{4} W_{\mu\nu} W^{\mu\nu} + \frac{1}{2} m_\phi^2 \phi_\mu \phi^\mu - \frac{1}{4} P_{\mu\nu} P^{\mu\nu} + \frac{1}{2} m_\rho^2 \boldsymbol{\rho}_\mu \cdot \boldsymbol{\rho}^\mu - \frac{1}{4} \mathbf{R}_{\mu\nu} \cdot \mathbf{R}^{\mu\nu} \\ & - U_{\text{NL}}(\sigma, \omega^\mu, \boldsymbol{\rho}^\mu) + \sum_\ell \bar{\psi}_\ell (i\gamma_\mu \partial^\mu - m_\ell) \psi_\ell, \end{aligned} \quad (1)$$

where $W_{\mu\nu} = \partial_\mu \omega_\nu - \partial_\nu \omega_\mu$, $P_{\mu\nu} = \partial_\mu \phi_\nu - \partial_\nu \phi_\mu$, and $\mathbf{R}_{\mu\nu} = \partial_\mu \boldsymbol{\rho}_\nu - \partial_\nu \boldsymbol{\rho}_\mu$ with $\psi_{B(\ell)}$ being the baryon (lepton) field, \mathbf{I}_B being the isospin matrix for baryon, and m_ℓ being the lepton mass. The sum B runs over the octet baryons, N (proton and neutron), Λ , $\Sigma^{+,0,-}$, and $\Xi^{0,-}$, and the sum ℓ is for the leptons, e^- and μ^- . The ω -, ϕ -, and ρ - B coupling constants are respectively denoted by $g_{\omega B}$, $g_{\phi B}$, and $g_{\rho B}$. The effective baryon mass, M_B^* , in matter is simply expressed as $M_B^*(\sigma, \sigma^*) = M_B - g_{\sigma B} \sigma - g_{\sigma^* B} \sigma^*$ with M_B being the mass in vacuum, and $g_{\sigma B}$ ($g_{\sigma^* B}$) being the σ - B (σ^* - B) coupling constant. Additionally, to obtain a quantitative description of nuclear ground-state properties, the minimum set of a nonlinear potential (Boguta & Bodmer 1977; Todd-Rutel & Piekarewicz 2005b; Miyatsu et al. 2013a; Hornick et al. 2018),

$$U_{\text{NL}}(\sigma, \omega^\mu, \boldsymbol{\rho}^\mu) = \frac{1}{3} g_2 \sigma^3 + \frac{1}{4} g_3 \sigma^4 - \Lambda_{\omega\rho} (\omega_\mu \omega^\mu) (\boldsymbol{\rho}_\mu \cdot \boldsymbol{\rho}^\mu), \quad (2)$$

is introduced in Equation (1). Here, the potential involves three coupling constants, g_2 , g_3 , and $\Lambda_{\omega\rho}$. In the present study, the hadron, meson, and lepton masses are taken as follows: $M_N = 939$ MeV, $M_\Lambda = 1116$ MeV, $M_\Sigma = 1193$ MeV, $M_\Xi = 1318$ MeV, $m_\sigma = 500$ MeV, $m_\omega = 783$ MeV, $m_\rho = 770$ MeV, $m_{\sigma^*} = 975$ MeV, $m_\phi = 1020$ MeV, $m_e = 0.511$ MeV, and $m_\mu = 105.7$ MeV.

In RMF approximation, the meson fields are replaced by the constant mean-field values: $\bar{\sigma}$, $\bar{\omega}$, $\bar{\sigma}^*$, $\bar{\phi}$ and $\bar{\rho}$ (the ρ^0 field). The equations of motion for the baryon and meson fields in uniform matter are thus given by

$$\left[i\gamma_\mu \partial^\mu - M_B^*(\bar{\sigma}, \bar{\sigma}^*) - g_{\omega B} \gamma_0 \bar{\omega} - g_{\phi B} \gamma_0 \bar{\phi} - g_{\rho B} \gamma_0 (\mathbf{I}_B)_3 \bar{\rho} \right] \Psi_B = 0, \quad (3)$$

$$m_\sigma^2 \bar{\sigma} + g_2 \bar{\sigma}^2 + g_3 \bar{\sigma}^3 = \sum_B g_{\sigma B} \rho_B^s, \quad (4)$$

$$m_{\sigma^*}^2 \bar{\sigma}^* = \sum_B g_{\sigma^* B} \rho_B^s, \quad (5)$$

$$(m_\omega^2 + 2\Lambda_{\omega\rho} \bar{\rho}^2) \bar{\omega} = \sum_B g_{\omega B} \rho_B, \quad (6)$$

$$m_\phi^2 \bar{\phi} = \sum_B g_{\phi B} \rho_B, \quad (7)$$

$$(m_\rho^2 + 2\Lambda_{\omega\rho} \bar{\omega}^2) \bar{\rho} = \sum_B g_{\rho B} (\mathbf{I}_B)_3 \rho_B, \quad (8)$$

where the scalar density, ρ_B^s , and the baryon density, ρ_B , read

$$\rho_B^s = \frac{1}{\pi^2} \int_0^{k_{FB}} dk \, k^2 \frac{M_B^*(\bar{\sigma}, \bar{\sigma}^*)}{\sqrt{k^2 + M_B^{*2}(\bar{\sigma}, \bar{\sigma}^*)}}, \quad \rho_B = \frac{k_{FB}^3}{3\pi^2}, \quad (9)$$

with k_{FB} being the Fermi momentum for baryon B .

With the self-consistent calculations of the meson fields given in Equations (4)–(8), the total energy density, ε , and pressure, P , in neutron-star matter are given by

$$\begin{aligned} \varepsilon = & \sum_B \frac{1}{\pi^2} \int_0^{k_{FB}} dk \, k^2 \sqrt{k^2 + M_B^{*2}(\bar{\sigma}, \bar{\sigma}^*)} + \sum_\ell \frac{1}{\pi^2} \int_0^{k_{F\ell}} dk \, k^2 \sqrt{k^2 + m_\ell^2}, \\ & + \frac{1}{2} m_\sigma^2 \bar{\sigma}^2 + \frac{1}{3} g_2 \bar{\sigma}^3 + \frac{1}{4} g_3 \bar{\sigma}^4 + \frac{1}{2} m_{\sigma^*}^2 \bar{\sigma}^{*2} + \frac{1}{2} m_\omega^2 \bar{\omega}^2 + \frac{1}{2} m_\phi^2 \bar{\phi}^2 + \frac{1}{2} m_\rho^2 \bar{\rho}^2 + 3\Lambda_{\omega\rho} \bar{\omega}^2 \bar{\rho}^2, \end{aligned} \quad (10)$$

$$\begin{aligned} P = & \frac{1}{3} \sum_B \frac{1}{\pi^2} \int_0^{k_{FB}} dk \, \frac{k^4}{\sqrt{k^2 + M_B^{*2}(\bar{\sigma}, \bar{\sigma}^*)}} + \frac{1}{3} \sum_\ell \frac{1}{\pi^2} \int_0^{k_{F\ell}} dk \, \frac{k^4}{\sqrt{k^2 + m_\ell^2}} \\ & - \frac{1}{2} m_\sigma^2 \bar{\sigma}^2 - \frac{1}{3} g_2 \bar{\sigma}^3 - \frac{1}{4} g_3 \bar{\sigma}^4 - \frac{1}{2} m_{\sigma^*}^2 \bar{\sigma}^{*2} + \frac{1}{2} m_\omega^2 \bar{\omega}^2 + \frac{1}{2} m_\phi^2 \bar{\phi}^2 + \frac{1}{2} m_\rho^2 \bar{\rho}^2 + \Lambda_{\omega\rho} \bar{\omega}^2 \bar{\rho}^2. \end{aligned} \quad (11)$$

3. NUMERICAL RESULTS AND DISCUSSIONS

We here present how to calibrate the nuclear EoS using the RMF model with a nonlinear potential. First, the coupling constants for nucleon (N) are determined so as to reproduce the saturation properties of nuclear matter from terrestrial experiments as well as theoretical calculations. And then, the calibrated EoSs are applied to the calculations of neutron-star matter, compared with the recent data of astrophysical observations, such as the maximum mass of a neutron star, M_{max} , and the tidal deformability of a canonical $1.4M_\odot$ neutron star, $\Lambda_{1.4}$. Especially, we focus on the effect of hyperons (Y) in the core of a neutron star. Finally, we give some constraints on the nuclear saturation

properties, which are not known well, so as to satisfy the data based on both nuclear experiments and astrophysical observations.

In order to deal with the properties of nuclear matter, it is very useful to consider the expansion of isospin asymmetric EoS with a power series in the isospin asymmetry, $\delta = (\rho_n - \rho_p)/n_B$, where the total baryon density is defined as $n_B = \sum_B \rho_B$ (Chen et al. 2009). The binding energy per nucleon is generally written as $E(n_B, \delta) = E_0(n_B) + E_{\text{sym}}(n_B)\delta^2 + \mathcal{O}(\delta^4)$, where $E_0(n_B)$ is the binding energy of symmetric nuclear matter and $E_{\text{sym}}(n_B)$ is the nuclear symmetry energy,

$$E_{\text{sym}}(n_B) = \frac{1}{2!} \frac{\partial^2 E(n_B, \delta)}{\partial \delta^2} \Big|_{\delta=0}. \quad (12)$$

Besides, $E_0(n_B)$ and $E_{\text{sym}}(n_B)$ can be expanded around the nuclear saturation density, n_0 , as

$$E_0(n_B) = E_0(n_0) + \frac{K_0}{2!} \chi^2 + \mathcal{O}(\chi^3), \quad (13)$$

$$E_{\text{sym}}(n_B) = E_{\text{sym}}(n_0) + L\chi + \frac{K_{\text{sym}}}{2!} \chi^2 + \mathcal{O}(\chi^3), \quad (14)$$

with $\chi = (n_B - n_0)/3n_0$ being a dimensionless variable characterizing the deviations of n_B from n_0 . The incompressibility coefficient of symmetric nuclear matter, K_0 , and the slope and curvature parameters of nuclear symmetry energy, L and K_{sym} , are respectively given by

$$K_0 = 9n_0^2 \frac{d^2 E_0(n_B)}{dn_B^2} \Big|_{n_B=n_0}, \quad L = 3n_0 \frac{dE_{\text{sym}}(n_B)}{dn_B} \Big|_{n_B=n_0}, \quad K_{\text{sym}} = 9n_0^2 \frac{d^2 E_{\text{sym}}(n_B)}{dn_B^2} \Big|_{n_B=n_0}. \quad (15)$$

3.1. Terrestrial experiments and theoretical calculations

The nuclear saturation properties have been extensively studied so far, and the binding energy per nucleon and nuclear symmetry energy at the saturation density, $E_0(n_0)$ and $E_{\text{sym}}(n_0)$, are determined with a highly accurate precision (Dutra et al. 2012, 2014; Baldo & Burgio 2016). However, the effective nucleon mass, M_N^* and the higher-order physical quantities, e.g. the incompressibility coefficient, K_0 , and the slope and curvature parameters, L and K_{sym} , still have a large ambiguity even at n_0 (Li & Han 2013; Zhang et al. 2018). As for the quantities, the recent standard values are hence employed as follows: we set $E_0 = -16.0$ MeV and $E_{\text{sym}} = 32.0$ MeV at $n_0 = 0.16 \text{ fm}^{-3}$, but M_N^* , K_0 , and L are supposed to be varied in the range of $0.50 \leq M_N^*/M_N \leq 0.80$, $180 \leq K_0 \text{ (MeV)} \leq 320$, and $30 \leq L \text{ (MeV)} \leq 100$, respectively.

The determining procedure of the coupling constants in the present study follows that in Miyatsu et al. (2013a): Using SU(3) flavor symmetry in the couplings of vector mesons to nucleons, the isoscalar coupling constants, $g_{\sigma N}$, $g_{\omega N}$, g_2 , and g_3 , are determined so as to reproduce E_0 , P , M_N^* and K_0 at n_0 with the assumption of $g_{\sigma^* N} = 0$. The values of a mixing angle, θ_v , and a ratio of the octet to singlet couplings, z , are, respectively, chosen to be $\theta_v = 37.50^\circ$ and $z = 0.1949$, which are the suggested values in the Nijmegen extended-soft-core (ESC) model (Rijken et al. 2010). Moreover, the coupling constants related to the isovector mesons, $g_{\rho N}$ and $\Lambda_{\omega\rho}$, are fixed to duplicate E_{sym} and L at n_0 .

In order to study a limit on M_N^* from the experiments and theoretical calculations, we consider the single-nucleon potential, U_N^{SEP} , based on the so-called Schrödinger-equivalent potential (SEP)

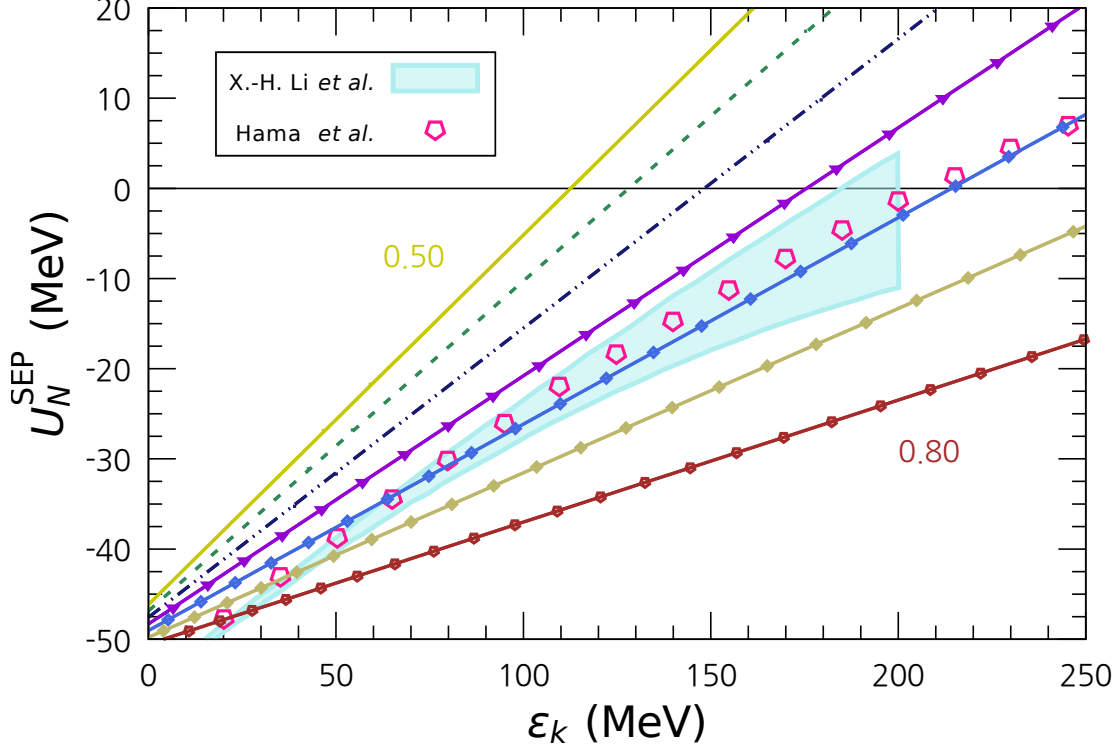


Figure 1. Energy dependence of single-nucleon potential, U_N^{SEP} , in symmetric nuclear matter at n_0 . We show the results for $M_N^*/M_N = 0.5\text{--}0.8$ by a 0.05 step. For details, see the text.

(Jaminon et al. 1981; Chen et al. 2007):

$$U_N^{\text{SEP}}(k, \varepsilon_k) = \Sigma_N^s(k) - \frac{E_N(k)}{M_N} \Sigma_N^0(k) + \frac{1}{2M_N} \left([\Sigma_N^s(k)]^2 - [\Sigma_N^0(k)]^2 \right), \quad (16)$$

where the nucleon kinetic energy, ε_k , reads $\varepsilon_k = E_N - M_N$ with E_N being the single-particle energy. The Lorentz-covariant scalar and vector self-energies for nucleon are respectively given by $\Sigma_N^s = -g_\sigma \bar{\sigma} - g_{\sigma^*} \bar{\sigma}^*$ and $\Sigma_N^0 = -g_\omega \bar{\omega} - g_\phi \bar{\phi} - g_\rho (\mathbf{I}_N)_3 \bar{\rho}$ with the meson fields in Equations (4)–(8). We show U_N^{SEP} in symmetric nuclear matter at n_0 with some experimental data in Figure 1. The shaded band reveals the results of nucleon-optical-model potential extracted from analyzing the nucleon-nucleus scattering data, denoted by X.-H. Li et al. (Li et al. 2013). We also include the results of U_N^{SEP} obtained by the Dirac phenomenology for elastic proton-nucleus scattering data calculated by Hama et al. (Hama et al. 1990). It is found that the satisfied values of M_N^* is roughly estimated to be $0.65 \leq M_N^*/M_N \leq 0.75$ in the current energy region. We note that the case of $M_N^*/M_N = 0.69$ is the optimum condition for satisfying the scattering data.

In Figure 2, the density dependence of E_{sym} and E_0 are depicted in the three cases of $M_N^*/M_N = 0.65, 0.70$, and 0.75 , which are deduced from the restriction of M_N^* shown in Figure 1. In Figure 2(a), we also present the experimental results obtained from heavy-ion collisions (Tsang et al. 2012; Russotto et al. 2016). It is found that E_{sym} strongly depends on L below n_0 , and L should be larger than 40 MeV to match the experimental data in all the cases. Because of the less dependence of K_0 , we only show the results in the case of $K_0 = 240$ MeV.

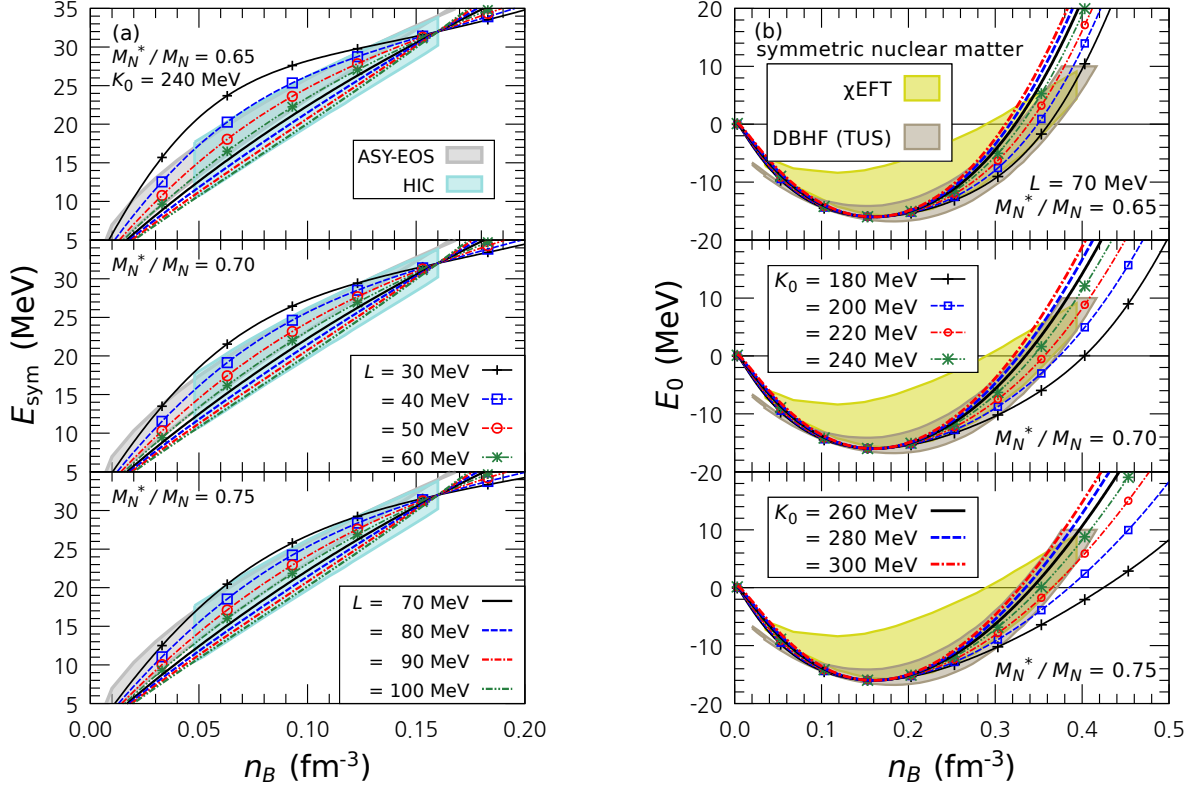


Figure 2. (a) Nuclear symmetry energy, E_{sym} , and (b) binding energy per nucleon, E_0 , as a function of n_B . In both upper (middle) [bottom] panels, we give the results in the case of $M_N^*/M_N = 0.65$ (0.70) [0.75]. The shaded bands in Figure (a) show the experimental data based on heavy-ion collisions, indicated by HIC and ASY-EOS (Tsang et al. 2012; Russotto et al. 2016). In Figure (b), we also present the theoretical results based on realistic N - N interactions using the Dirac-Brueckner-Hartree-Fock (DBHF) calculation (Katayama & Saito 2013) or the chiral effective field theory (χ EFT) (Sammarruca et al. 2015).

The E_0 in the intermediate density region is presented in Figure 2(b), where K_0 varies from 180 MeV to 300 MeV. Although the difference among the results with various K_0 is not so large below n_0 , E_0 is sensitive to K_0 and M_N^* above n_0 . On the other hand, since L has little influence on E_0 , we only show the results in the case of $L = 70$ MeV, which is a middle value in the acceptable range of L explained in Figure 2(a). Compared with the realistic calculations in the Dirac-Brueckner-Hartree-Fock (DBHF) theory (Katayama & Saito 2013) and the chiral effective field theory (χ EFT) (Sammarruca et al. 2015), it is possible to impose some constraints on the nuclear EoSs at higher densities. We find that the allowed range of K_0 can be restricted to be $180 \leq K_0$ (MeV) ≤ 230 , $210 \leq K_0$ (MeV) ≤ 270 , and $235 \leq K_0$ (MeV) ≤ 305 for $M_N^*/M_N = 0.65$, 0.70 , and 0.75 , respectively.

3.2. Astrophysical observations of neutron stars

The characteristics of a neutron star are, in general, estimated by solving the Tolman-Oppenheimer-Volkoff (TOV) equation with the EoS for neutron-star matter in which the charge neutrality and β equilibrium under weak processes are imposed (Tolman 1934; Oppenheimer & Volkoff 1939). Since the radius of a neutron star is remarkably sensitive to the EoS at very low densities, we adopt the EoS for nonuniform matter below $n_B = 0.068 \text{ fm}^{-3}$, where nuclei are taken into account using the

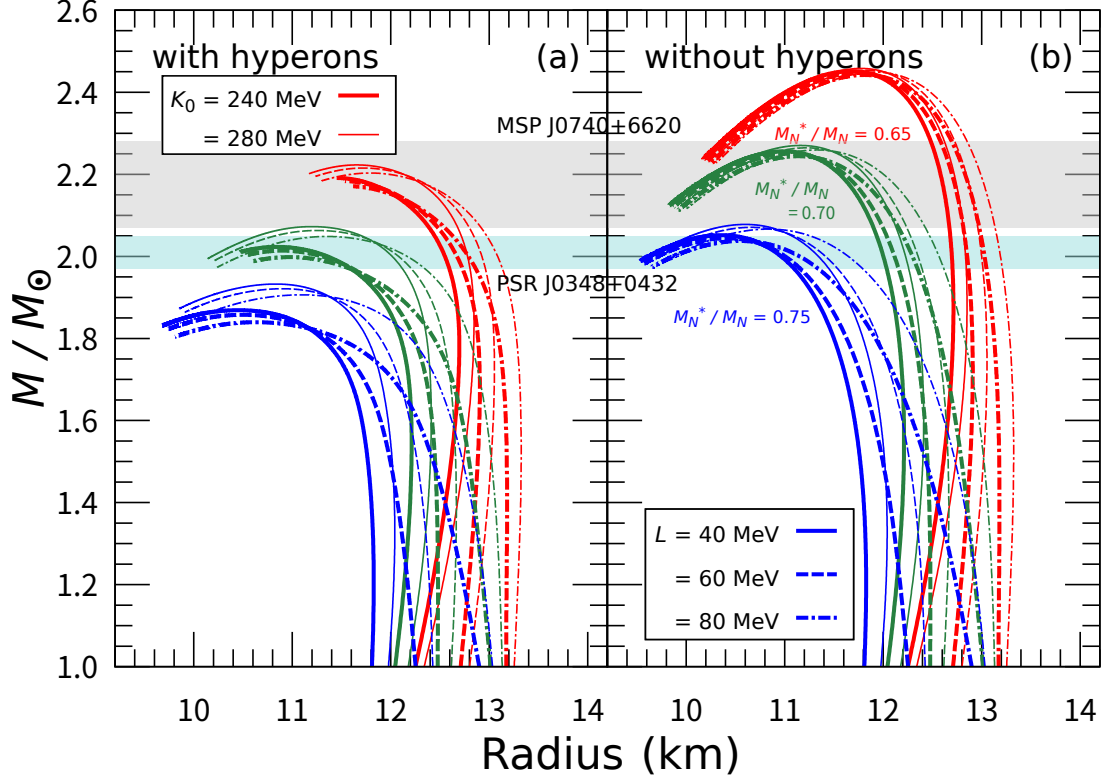


Figure 3. Mass-radius relations of a neutron star (a) with or (b) without hyperons in the various combinations of M_N^*/M_N , L , and K_0 . In both panels, the red (green) [blue] line corresponds to the case of $M_N^*/M_N = 0.65$ (0.70) [0.75], the solid (dashed) [dotted-dashed] line is for $L = 40$ (60) [80] MeV, and the case of $K_0 = 240$ (280) MeV is given by the thick (thin) line. The shaded bands also show the observation data of PSR J0348+0432 ($2.01 \pm 0.04 M_\odot$) and MSP J0740+6620 ($2.14^{+0.10}_{-0.09} M_\odot$) (Antoniadis et al. 2013; Cromartie et al. 2019).

Thomas-Fermi calculation (Miyatsu et al. 2013b). Moreover, the coupling constants for hyperons are determined so as to fit the experimental data of hypernuclei and the Nagara event in SU(3) flavor symmetry: $U_\Lambda^{(N)} = -28$ MeV, $U_\Sigma^{(N)} = +30$ MeV, $U_\Xi^{(N)} = -18$ MeV, and $U_\Lambda^{(\Lambda)} \simeq -5$ MeV, with $U_Y^{(j)}$ being the potential depth for Y in matter of the baryon species j (Schaffner & Mishustin 1996; Takahashi et al. 2001; Yang & Shen 2008; Miyatsu et al. 2013a). As for a potential depth for Y , we employ U_Y^{SEP} given in Equation (16).

The mass-radius relations of a neutron star with and without hyperons are presented in Figure 3. As is well known, if hyperons are taken into account in the core, the maximum mass of a neutron star, M_{max} , is reduced drastically. Thus, in order to explain the observed masses of heavy neutron stars (Antoniadis et al. 2013; Cromartie et al. 2019), it is possible to give more severe constraints on the neutron-star EoSs by considering hyperons. It is found that M_{max} is very sensitive to M_N^* at n_0 , and the EoSs for $M_N^*/M_N > 0.70$ are ruled out by the observation data once hyperons are included. If we combine both restrictions of M_{max} (with hyperons) and U_N^{SEP} , shown in Figure 1, we can estimate the more refined condition of M_N^* to be $0.65 \leq M_N^*/M_N \leq 0.70$ at n_0 . Meanwhile, L and K_0 have a small impact on M_{max} , and they rather affect the neutron-star radius.

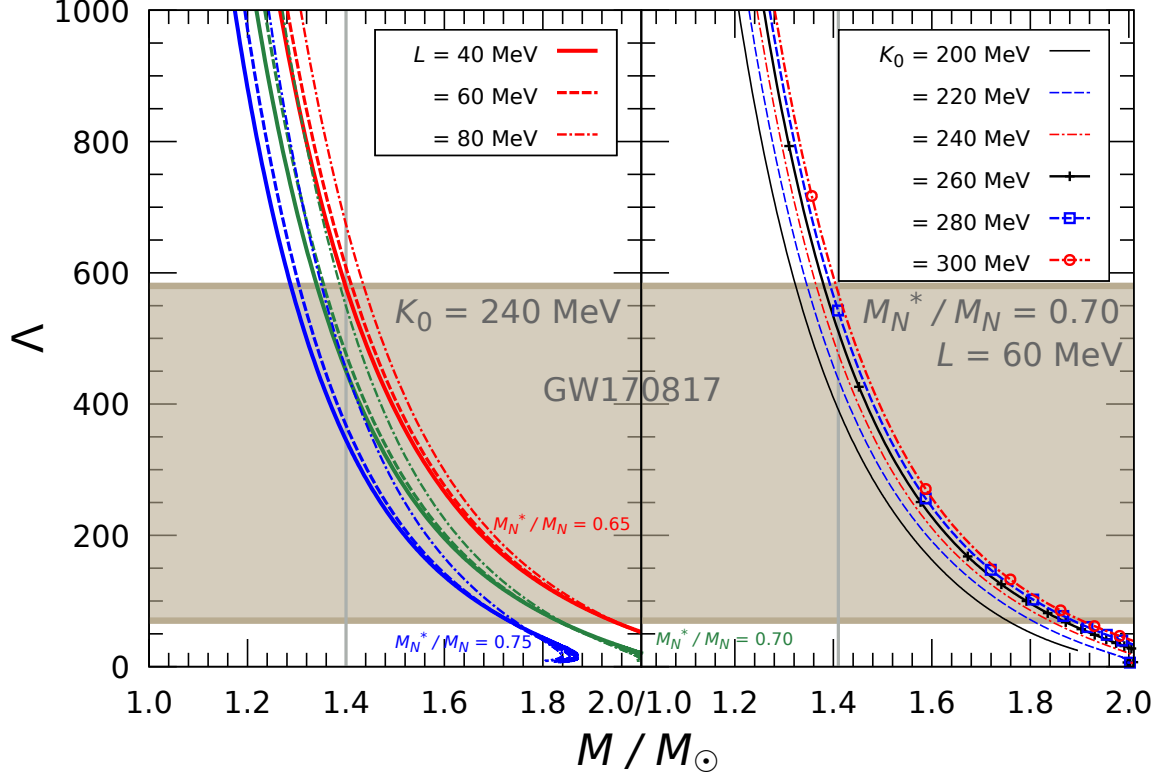


Figure 4. Tidal deformability of a neutron star with hyperons, Λ , as a function of M/M_\odot . The panel (a) shows the influence of M_N^*/M_N and L for $K_0 = 240$ MeV, and the panel (b) expresses the dependence of K_0 for $M_N^*/M_N = 0.70$ and $L = 60$ MeV. The shaded band also shows the astrophysical constraint on the tidal deformability of a canonical $1.4M_\odot$ neutron star from the merger event, GW170817 ($70 < \Lambda_{1.4} < 580$) (Abbott et al. 2018).

In Figure 4, the dimensionless tidal deformability of a neutron star with hyperons, Λ , is presented with the astrophysical constraint on the GW signals from binary neutron star merger, GW170817, detected by the advanced LIGO and advanced Virgo observatories (Abbott et al. 2018, 2019). Hereafter, hyperons are taken into account in all the calculations. With the observation data, it is possible to impose constraints on the EoSs for neutron stars using the tidal deformability of a canonical $1.4M_\odot$ neutron star, $\Lambda_{1.4}$. It is found that Λ becomes small as M_N^* at n_0 increases, but the larger L , which gives the larger radius of a neutron star shown in Figure 3, consequently brings the larger Λ as shown in Figure 4(a). We also see that, in Figure 4(b), there is a strong correlation between K_0 and Λ , and the smaller K_0 is preferred to support the astrophysical data of $\Lambda_{1.4}$.

The contour lines of M_{max} in the K_0 – L plane are presented in Figure 5. In Figure 5(a), we show several lines of M_{max}/M_\odot in the case of $M_N^*/M_N = 0.69$, which is the favorable condition for supporting U_N^{SEP} as already explained in Figure 1. It is found that M_{max} is sensitive to K_0 , while L has a little influence on M_{max} . The larger K_0 and the smaller L are required to support the heavier M_{max} , and thus the preferable correlation between K_0 and L is restricted in the right-hand region above the yellow line of $M_{\text{max}}/M_\odot = 2.01$ to explain the observed mass of PSR J0348+0432 (Antoniadis et al. 2013). In addition, the effect of M_N^*/M_N at n_0 on M_{max}/M_\odot is depicted in Figure 5(b). We find that the smaller M_N^* can easily satisfy the $2M_\odot$ constraint with the smaller K_0 , while

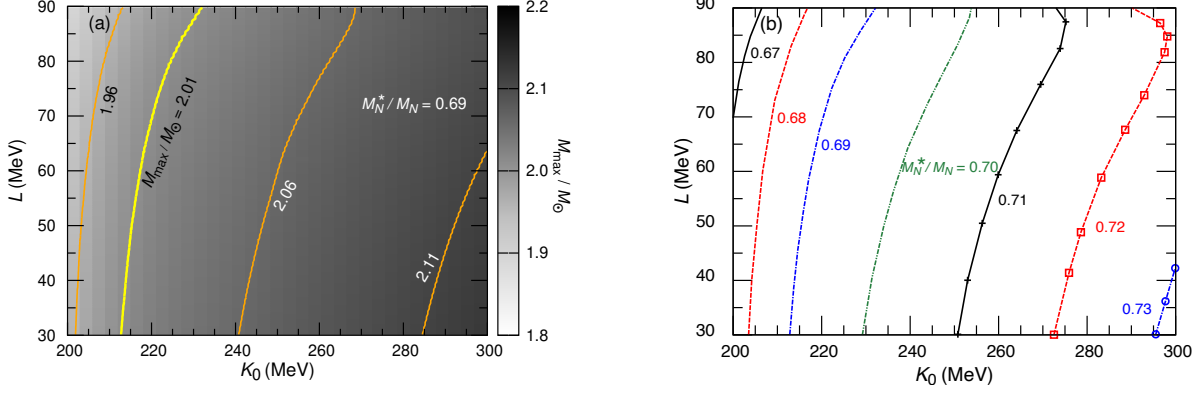


Figure 5. Schematic representation of M_{\max} in the K_0 – L plane. We show (a) M_{\max}/M_{\odot} for $M_N^*/M_N = 0.69$, and (b) M_N^*/M_N for $M_{\max}/M_{\odot} = 2.01$. For details, see the text.

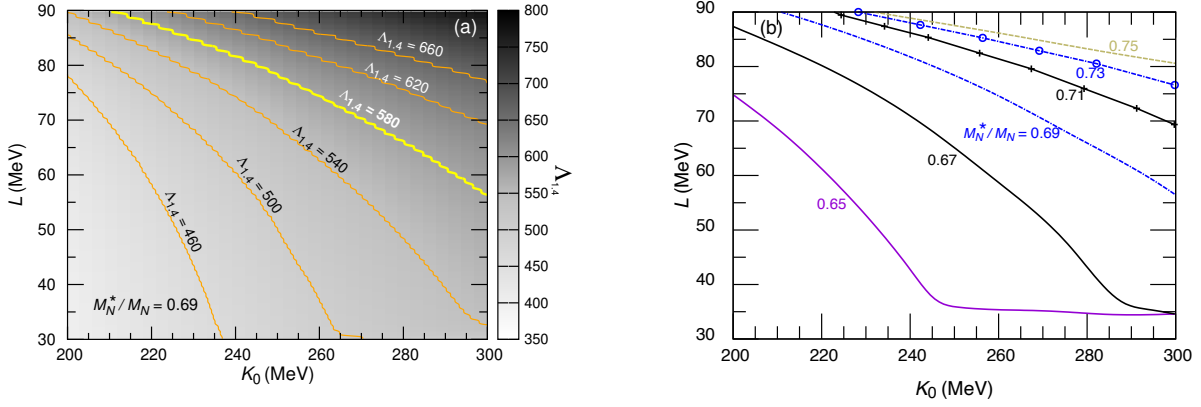


Figure 6. Same as Figure 5, but for $\Lambda_{1.4}$. We show (a) $\Lambda_{1.4}$ for $M_N^*/M_N = 0.69$, and (b) M_N^*/M_N for $\Lambda_{1.4} = 580$. For details, see the text.

the larger K_0 is needed as M_N^* increases. We here emphasize that owing to the softness of the EoSs for neutron stars with hyperons in the core, it is possible to impose a stringent constraint on the correlation between K_0 and L .

In Figure 6, we also present the schematic representation of $\Lambda_{1.4}$ in the K_0 – L plane. Each line indicates the specific values of $\Lambda_{1.4}$ for $M_N^*/M_N = 0.69$ in Figure 6(a). It is found that $\Lambda_{1.4}$ is quite sensitive to K_0 and L and, for example, the larger K_0 and L lead to the larger $\Lambda_{1.4}$. According to the upper limit based on the GW signals, $\Lambda_{1.4} = 580$ (Abbott et al. 2018), the region below the yellow line can be permitted. Moreover, in Figure 6(b), we consider the influence of M_N^*/M_N on $\Lambda_{1.4}$ in the K_0 – L plane, focusing the upper boundary of $\Lambda_{1.4}$. As M_N^* decreases, L becomes sensitive to $\Lambda_{1.4}$ compared to K_0 . We note that, contrary to the case of M_{\max} shown in Figure 5, the existence of hyperons in the core of a neutron star does not affect $\Lambda_{1.4}$ because hyperons do not have any influence on the radii of neutron stars as shown in Figure 3.

3.3. Constraints on nuclear saturation properties

By combining the results obtained from the calculations of nuclear and neutron-star matter, we put restrictions on the nuclear properties at n_0 . In Figure 7(a), we show the constrained parameter region

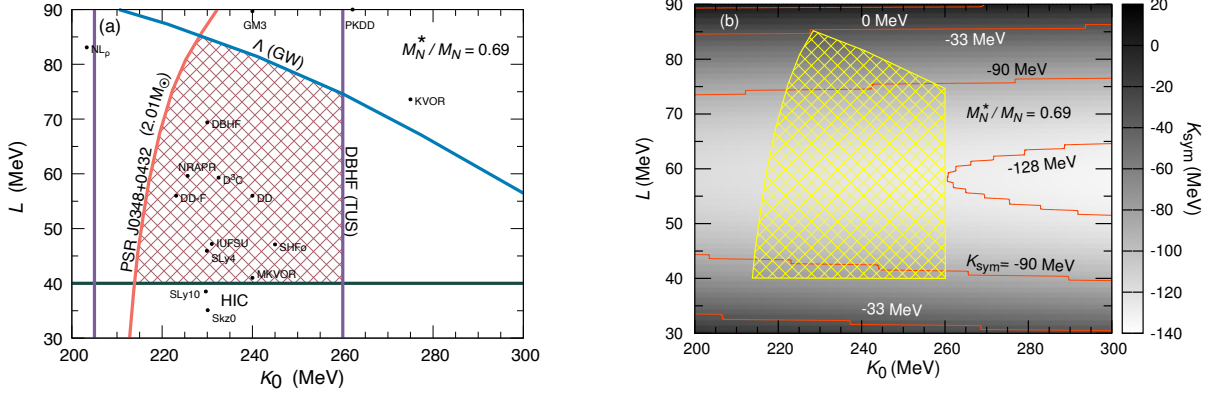


Figure 7. (a) Allowed parameter region in the K_0 - L plane, and (b) constraint on K_{sym} for $M_N^*/M_N = 0.69$ in the case of $M_{\text{max}}/M_\odot = 2.01$. We also show some results calculated by realistic nuclear models in the panel (a) (Dutra et al. 2012, 2014; Tews et al. 2017).

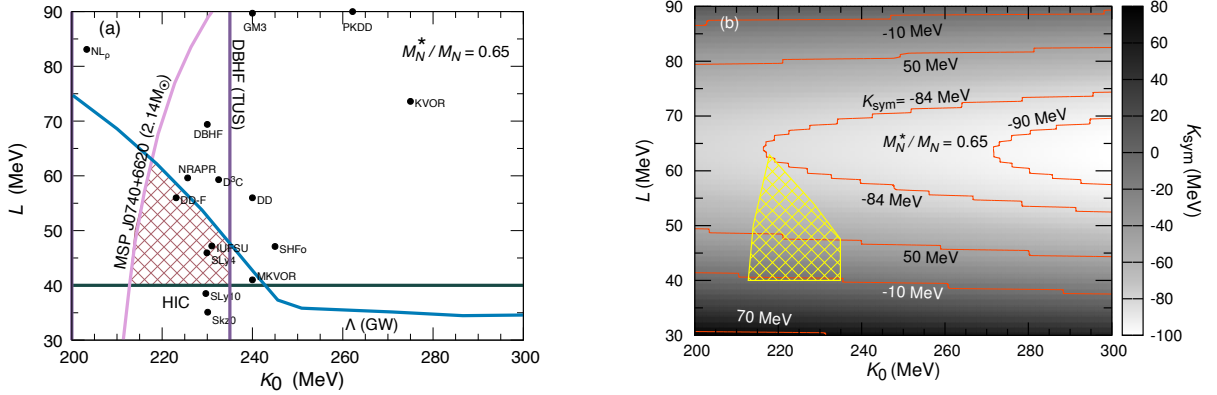


Figure 8. Same as Figure 7, but for $M_N^*/M_N = 0.65$ in the case of $M_{\text{max}}/M_\odot = 2.14$.

in the K_0 - L plane for $M_N^*/M_N = 0.69$, which is the best fitted value for reproducing U_N^{SEP} at n_0 . As explained in Figure 2, the lowest limit of L is presented by the data of HIC analysis based on terrestrial experiments, and K_0 is theoretically constrained by the DBHF (TUS) calculations. Moreover, we see that M_{max} of PSR J0348+0432 and Λ of GW signals, which are based on astrophysical observations, are very useful to give constraints on the relations between K_0 and L . In addition, it is possible to restrict K_{sym} using the closed, meshed region of K_0 and L in Figure 7(b). It is found that the satisfied ranges of K_0 and L can be respectively estimated to be $215 \leq K_0$ (MeV) ≤ 260 and $40 \leq L$ (MeV) ≤ 85 , and the corresponding value of K_{sym} roughly lies in the range of $-128 \leq K_{\text{sym}}$ (MeV) ≤ -33 , which is more severe than that of extensive surveys of over 520 theoretical predictions, $-400 \leq K_{\text{sym}}$ (MeV) ≤ 100 (Dutra et al. 2012, 2014; Li & Magno 2020). The present result is almost the same as the constraints calculated by Malik et al. (2018), $-113 \leq K_{\text{sym}}$ (MeV) ≤ -52 and $-141 \leq K_{\text{sym}}$ (MeV) ≤ 16 .

Figure 8 shows another acceptable parameter region using the more massive neutron-star condition, $M_{\text{max}}/M_\odot = 2.14$, for $M_N^*/M_N = 0.65$. If the heavier mass of a observed neutron star, MSP J0740+6620, is taken into account, then the parameter region is further restricted, and K_0 and L are respectively estimated to be $215 \leq K_0$ (MeV) ≤ 235 and $40 \leq L$ (MeV) ≤ 65 in Figure 8(a).

Consequently, the more stringent constraint on K_{sym} is given to be $-84 \leq K_{\text{sym}} \text{ (MeV)} \leq -10$ in Figure 8(b).

4. SUMMARY

We have studied the properties of nuclear and neutron-star matter using the RMF model with a nonlinear potential. In order to restrict the EoS for isospin-asymmetric nuclear matter in the extensive density region, the terrestrial experiments and the recent astrophysical observations of neutron stars and GW signals have been taken into account. Moreover, we have investigated the effects of important physical quantities, namely M_N^* , K_0 , and L , which are still unknown even at n_0 .

As for the analyses of nuclear properties in the density region below $n_B = 0.5 \text{ fm}^{-3}$, we have employed the data based on some nuclear experiments and theoretical results. We have found that M_N^* at n_0 is roughly estimated to be $0.65 \leq M_N^*/M_N \leq 0.75$ so as to reproduce U_N^{SEP} obtained from the nucleon-nucleus and elastic proton-nucleus scattering data (Li et al. 2013; Hama et al. 1990). It has been also found that E_{sym} strongly depends on L below n_0 , and L should be larger than 40 MeV to satisfy the experimental results obtained from heavy-ion collisions (Tsang et al. 2012; Russotto et al. 2016). In addition, compared with the realistic calculations based on the DBHF theory and the χ EFT (Katayama & Saito 2013; Sammarruca et al. 2015), K_0 can be restricted to be $180 \leq K_0 \text{ (MeV)} \leq 230$, $210 \leq K_0 \text{ (MeV)} \leq 270$, and $235 \leq K_0 \text{ (MeV)} \leq 305$ in the cases of $M_N^*/M_N = 0.65$, 0.70, and 0.75, respectively.

Concerning the neutron-star calculations, we have adopted the astrophysical constraints on M_{max} and $\Lambda_{1.4}$ (Antoniadis et al. 2013; Cromartie et al. 2019; Abbott et al. 2018, 2019). We have also considered the existence of hyperons in the core to restrict the realistic EoS for neutron stars using SU(3) flavor symmetry (Miyatsu et al. 2012, 2013a; Katayama et al. 2012; Weissenborn et al. 2012). It has been found that M_{max} is very sensitive to M_N^* at n_0 , and the neutron-star EoSs in the cases of $M_N^*/M_N > 0.70$ are ruled out to support $2M_\odot$ neutron stars with hyperons. Additionally, we have found a strong correlation between K_0 and Λ , and the smaller K_0 is preferred to satisfy the astrophysical data of $\Lambda_{1.4}$.

At last, by combining both calculations of nuclear and neutron-star matter, we have presented the constrained relations between K_0 and L in Figures 7 and 8. It has been found that, in the case of $M_N^*/M_N = 0.69$ and $M_{\text{max}}/M_\odot = 2.01$, K_0 and L can be respectively estimated to be $215 \leq K_0 \text{ (MeV)} \leq 260$ and $40 \leq L \text{ (MeV)} \leq 85$, and the corresponding value of K_{sym} roughly lies in the range of $-128 \leq K_{\text{sym}} \text{ (MeV)} \leq -33$. If we consider the higher limit of a neutron-star mass, it can be possible to impose severe constraints on K_0 , L , and K_{sym} .

In conclusion, it has been found that the astrophysical information of massive neutron stars and tidal deformabilities as well as the terrestrial nuclear experimental data plays an important role to restrict the EoS for neutron stars. Especially, the softness of the nuclear EoS due to the existence of hyperons in the core gives stringent constraints on the physical quantities, K_0 , L , and K_{sym} . Since the other exotic degrees of freedom in the core of a neutron star and/or the phase transition from hadrons to quarks may influence M_{max} and $\Lambda_{1.4}$ (Alford et al. 2013; Miyatsu et al. 2015; Han & Steiner 2019), we have to include their effects as well as hyperons. We leave them for the future works.

ACKNOWLEDGMENTS

This work was supported by JSPS KAKENHI Grant Number JP17K14298 and by the National Research Foundation of Korea (Grant Nos. NRF-2020R1A2C3006177 and NRF-2013M7A1A1075764).

REFERENCES

- Abbott, B., et al. 2018, *Phys. Rev. Lett.*, 121, 161101, doi: [10.1103/PhysRevLett.121.161101](https://doi.org/10.1103/PhysRevLett.121.161101)
- . 2019, *Phys. Rev. X*, 9, 011001, doi: [10.1103/PhysRevX.9.011001](https://doi.org/10.1103/PhysRevX.9.011001)
- Alford, M. G., Han, S., & Prakash, M. 2013, *Phys. Rev. D*, 88, 083013, doi: [10.1103/PhysRevD.88.083013](https://doi.org/10.1103/PhysRevD.88.083013)
- Annala, E., Gorda, T., Kurkela, A., & Vuorinen, A. 2018, *Phys. Rev. Lett.*, 120, 172703, doi: [10.1103/PhysRevLett.120.172703](https://doi.org/10.1103/PhysRevLett.120.172703)
- Antoniadis, J., et al. 2013, *Science*, 340, 6131, doi: [10.1126/science.1233232](https://doi.org/10.1126/science.1233232)
- Arzoumanian, Z., et al. 2018, *Astrophys. J. Suppl.*, 235, 37, doi: [10.3847/1538-4365/aab5b0](https://doi.org/10.3847/1538-4365/aab5b0)
- Baldo, M., & Burgio, G. F. 2016, *Prog. Part. Nucl. Phys.*, 91, 203, doi: [10.1016/j.ppnp.2016.06.006](https://doi.org/10.1016/j.ppnp.2016.06.006)
- Boguta, J., & Bodmer, A. R. 1977, *Nucl. Phys.*, A292, 413, doi: [10.1016/0375-9474\(77\)90626-1](https://doi.org/10.1016/0375-9474(77)90626-1)
- Capano, C. D., Tews, I., Brown, S. M., et al. 2020, *Nature Astron.*, 4, 625, doi: [10.1038/s41550-020-1014-6](https://doi.org/10.1038/s41550-020-1014-6)
- Chatziioannou, K., Haster, C.-J., & Zimmerman, A. 2018, *Phys. Rev. D*, 97, 104036, doi: [10.1103/PhysRevD.97.104036](https://doi.org/10.1103/PhysRevD.97.104036)
- Chen, L.-W., Cai, B.-J., Ko, C. M., et al. 2009, *Phys. Rev.*, C80, 014322, doi: [10.1103/PhysRevC.80.014322](https://doi.org/10.1103/PhysRevC.80.014322)
- Chen, L.-W., Ko, C. M., & Li, B.-A. 2007, *Phys. Rev.*, C76, 054316, doi: [10.1103/PhysRevC.76.054316](https://doi.org/10.1103/PhysRevC.76.054316)
- Cromartie, H. T., et al. 2019, *Nature Astron.*, 4, 72, doi: [10.1038/s41550-019-0880-2](https://doi.org/10.1038/s41550-019-0880-2)
- Danielewicz, P., & Lee, J. 2009, *Nucl. Phys. A*, 818, 36, doi: [10.1016/j.nuclphysa.2008.11.007](https://doi.org/10.1016/j.nuclphysa.2008.11.007)
- De, S., Finstad, D., Lattimer, J. M., et al. 2018, *Phys. Rev. Lett.*, 121, 091102, doi: [10.1103/PhysRevLett.121.091102](https://doi.org/10.1103/PhysRevLett.121.091102)
- Demorest, P., Pennucci, T., Ransom, S., Roberts, M., & Hessels, J. 2010, *Nature*, 467, 1081, doi: [10.1038/nature09466](https://doi.org/10.1038/nature09466)
- Dutra, M., Lourenco, O., Sa Martins, J. S., et al. 2012, *Phys. Rev.*, C85, 035201, doi: [10.1103/PhysRevC.85.035201](https://doi.org/10.1103/PhysRevC.85.035201)
- Dutra, M., Lourenço, O., Avancini, S. S., et al. 2014, *Phys. Rev.*, C90, 055203, doi: [10.1103/PhysRevC.90.055203](https://doi.org/10.1103/PhysRevC.90.055203)
- Fattoyev, F., Horowitz, C., Piekarewicz, J., & Shen, G. 2010, *Phys. Rev. C*, 82, 055803, doi: [10.1103/PhysRevC.82.055803](https://doi.org/10.1103/PhysRevC.82.055803)
- Fattoyev, F. J., Piekarewicz, J., & Horowitz, C. J. 2018, *Phys. Rev. Lett.*, 120, 172702, doi: [10.1103/PhysRevLett.120.172702](https://doi.org/10.1103/PhysRevLett.120.172702)
- Fortin, M., Raduta, A. R., Avancini, S., & Providência, C. 2020, *Phys. Rev. D*, 101, 034017, doi: [10.1103/PhysRevD.101.034017](https://doi.org/10.1103/PhysRevD.101.034017)
- Glendenning, N. 1997, *Compact stars: Nuclear physics, particle physics, and general relativity*
- Glendenning, N., & Moszkowski, S. 1991, *Phys. Rev. Lett.*, 67, 2414, doi: [10.1103/PhysRevLett.67.2414](https://doi.org/10.1103/PhysRevLett.67.2414)
- Hama, S., Clark, B. C., Cooper, E. D., Sherif, H. S., & Mercer, R. L. 1990, *Phys. Rev.*, C41, 2737, doi: [10.1103/PhysRevC.41.2737](https://doi.org/10.1103/PhysRevC.41.2737)
- Han, S., & Steiner, A. W. 2019, *Phys. Rev. D*, 99, 083014, doi: [10.1103/PhysRevD.99.083014](https://doi.org/10.1103/PhysRevD.99.083014)
- Hewish, A., Bell, S., Pilkington, J., Scott, P., & Collins, R. 1968, *Nature*, 217, 709, doi: [10.1038/217709a0](https://doi.org/10.1038/217709a0)
- Hewish, A., & Okoye, S. E. 1965, *Nature*, 207, 59, doi: [10.1038/207059a0](https://doi.org/10.1038/207059a0)
- Hinderer, T. 2008, *Astrophys. J.*, 677, 1216, doi: [10.1086/533487](https://doi.org/10.1086/533487)
- Hinderer, T., Lackey, B. D., Lang, R. N., & Read, J. S. 2010, *Phys. Rev. D*, 81, 123016, doi: [10.1103/PhysRevD.81.123016](https://doi.org/10.1103/PhysRevD.81.123016)
- Hornick, N., Tolos, L., Zacchi, A., Christian, J.-E., & Schaffner-Bielich, J. 2018, *Phys. Rev.*, C98, 065804, doi: [10.1103/PhysRevC.98.065804](https://doi.org/10.1103/PhysRevC.98.065804)
- Jaminon, M., Mahaux, C., & Rochus, P. 1981, *Nucl. Phys.*, A365, 371, doi: [10.1016/0375-9474\(81\)90397-3](https://doi.org/10.1016/0375-9474(81)90397-3)

- Katayama, T., Miyatsu, T., & Saito, K. 2012, *Astrophys. J. Suppl.*, 203, 22, doi: [10.1088/0067-0049/203/2/22](https://doi.org/10.1088/0067-0049/203/2/22)
- Katayama, T., & Saito, K. 2013, *Phys. Rev. C*, 88, 035805, doi: [10.1103/PhysRevC.88.035805](https://doi.org/10.1103/PhysRevC.88.035805)
- Kim, Y.-M., Lim, Y., Kwak, K., Hyun, C. H., & Lee, C.-H. 2018, *Phys. Rev. C*, 98, 065805, doi: [10.1103/PhysRevC.98.065805](https://doi.org/10.1103/PhysRevC.98.065805)
- Krastev, P. G., & Li, B.-A. 2019, *Comments Nucl. Part. Phys.*, 46, 074001, doi: [10.1088/1361-6471/ab1a7a](https://doi.org/10.1088/1361-6471/ab1a7a)
- Kumar, B., Biswal, S., & Patra, S. 2017, *Phys. Rev. C*, 95, 015801, doi: [10.1103/PhysRevC.95.015801](https://doi.org/10.1103/PhysRevC.95.015801)
- Lattimer, J. M., & Prakash, M. 2007, *Phys. Rept.*, 442, 109, doi: [10.1016/j.physrep.2007.02.003](https://doi.org/10.1016/j.physrep.2007.02.003)
- Li, B.-A., Chen, L.-W., & Ko, C. M. 2008, *Phys. Rept.*, 464, 113, doi: [10.1016/j.physrep.2008.04.005](https://doi.org/10.1016/j.physrep.2008.04.005)
- Li, B.-A., & Han, X. 2013, *Phys. Lett.*, B727, 276, doi: [10.1016/j.physletb.2013.10.006](https://doi.org/10.1016/j.physletb.2013.10.006)
- Li, B.-A., Krastev, P. G., Wen, D.-H., & Zhang, N.-B. 2019, *Eur. Phys. J. A*, 55, 117, doi: [10.1140/epja/i2019-12780-8](https://doi.org/10.1140/epja/i2019-12780-8)
- Li, B.-A., & Magno, M. 2020, *Phys. Rev. C*, 102, 045807, doi: [10.1103/PhysRevC.102.045807](https://doi.org/10.1103/PhysRevC.102.045807)
- Li, B.-A., Ramos, A., Verde, G., & Vidana, I. 2014, *Eur. Phys. J. A*, 50, 9, doi: [10.1140/epja/i2014-14009-x](https://doi.org/10.1140/epja/i2014-14009-x)
- Li, C.-M., Yan, Y., Geng, J.-J., Huang, Y.-F., & Zong, H.-S. 2018, *Phys. Rev. D*, 98, 083013, doi: [10.1103/PhysRevD.98.083013](https://doi.org/10.1103/PhysRevD.98.083013)
- Li, J. J., & Sedrakian, A. 2019, *Astrophys. J. Lett.*, 874, L22, doi: [10.3847/2041-8213/ab1090](https://doi.org/10.3847/2041-8213/ab1090)
- Li, X.-H., Cai, B.-J., Chen, L.-W., et al. 2013, *Phys. Lett.*, B721, 101, doi: [10.1016/j.physletb.2013.03.005](https://doi.org/10.1016/j.physletb.2013.03.005)
- Lim, Y., & Holt, J. W. 2018, *Phys. Rev. Lett.*, 121, 062701, doi: [10.1103/PhysRevLett.121.062701](https://doi.org/10.1103/PhysRevLett.121.062701)
- Lourenço, O., Dutra, M., Lenzi, C. H., Flores, C. V., & Menezes, D. P. 2019, *Phys. Rev. C*, 99, 045202, doi: [10.1103/PhysRevC.99.045202](https://doi.org/10.1103/PhysRevC.99.045202)
- Malik, T., Alam, N., Fortin, M., et al. 2018, *Phys. Rev. C*, 98, 035804, doi: [10.1103/PhysRevC.98.035804](https://doi.org/10.1103/PhysRevC.98.035804)
- Miyatsu, T., Cheoun, M.-K., Ishizuka, C., et al. 2020, *Phys. Lett. B*, 803, 135282, doi: [10.1016/j.physletb.2020.135282](https://doi.org/10.1016/j.physletb.2020.135282)
- Miyatsu, T., Cheoun, M.-K., & Saito, K. 2013a, *Phys. Rev.*, C88, 015802, doi: [10.1103/PhysRevC.88.015802](https://doi.org/10.1103/PhysRevC.88.015802)
- . 2015, *Astrophys. J.*, 813, 135, doi: [10.1088/0004-637X/813/2/135](https://doi.org/10.1088/0004-637X/813/2/135)
- Miyatsu, T., Katayama, T., & Saito, K. 2012, *Phys. Lett. B*, 709, 242, doi: [10.1016/j.physletb.2012.02.009](https://doi.org/10.1016/j.physletb.2012.02.009)
- Miyatsu, T., Yamamuro, S., & Nakazato, K. 2013b, *Astrophys. J.*, 777, 4, doi: [10.1088/0004-637X/777/1/4](https://doi.org/10.1088/0004-637X/777/1/4)
- Most, E. R., Weih, L. R., Rezzolla, L., & Schaffner-Bielich, J. 2018, *Phys. Rev. Lett.*, 120, 261103, doi: [10.1103/PhysRevLett.120.261103](https://doi.org/10.1103/PhysRevLett.120.261103)
- Oppenheimer, J., & Volkoff, G. 1939, *Phys. Rev.*, 55, 374, doi: [10.1103/PhysRev.55.374](https://doi.org/10.1103/PhysRev.55.374)
- Paschalidis, V., Yagi, K., Alvarez-Castillo, D., Blaschke, D. B., & Sedrakian, A. 2018, *Phys. Rev. D*, 97, 084038, doi: [10.1103/PhysRevD.97.084038](https://doi.org/10.1103/PhysRevD.97.084038)
- Radice, D., Perego, A., Zappa, F., & Bernuzzi, S. 2018, *Astrophys. J. Lett.*, 852, L29, doi: [10.3847/2041-8213/aaa402](https://doi.org/10.3847/2041-8213/aaa402)
- Raithel, C., Özel, F., & Psaltis, D. 2018, *Astrophys. J. Lett.*, 857, L23, doi: [10.3847/2041-8213/aabcbf](https://doi.org/10.3847/2041-8213/aabcbf)
- Raithel, C. A., & Özel, F. 2019, *Astrophys. J.*, 885, 121, doi: [10.3847/1538-4357/ab48e6](https://doi.org/10.3847/1538-4357/ab48e6)
- Ribes, P., Ramos, A., Tolos, L., Gonzalez-Boquera, C., & Centelles, M. 2019, *Astrophys. J.*, 883, 168, doi: [10.3847/1538-4357/ab3a93](https://doi.org/10.3847/1538-4357/ab3a93)
- Rijken, T. A., Nagels, M. M., & Yamamoto, Y. 2010, *Prog. Theor. Phys. Suppl.*, 185, 14, doi: [10.1143/PTPS.185.14](https://doi.org/10.1143/PTPS.185.14)
- Russotto, P., et al. 2016, *Phys. Rev. C*, 94, 034608, doi: [10.1103/PhysRevC.94.034608](https://doi.org/10.1103/PhysRevC.94.034608)
- Sahoo, H. S., Mishra, R., Mohanty, D. K., Panda, P. K., & Barik, N. 2019, *Phys. Rev. C*, 99, 055803, doi: [10.1103/PhysRevC.99.055803](https://doi.org/10.1103/PhysRevC.99.055803)
- Sammarruca, F., Coraggio, L., Holt, J., et al. 2015, *Phys. Rev. C*, 91, 054311, doi: [10.1103/PhysRevC.91.054311](https://doi.org/10.1103/PhysRevC.91.054311)
- Schaffner, J., & Mishustin, I. N. 1996, *Phys. Rev. C*, 53, 1416, doi: [10.1103/PhysRevC.53.1416](https://doi.org/10.1103/PhysRevC.53.1416)
- Schaffner-Bielich, J. 2008, *Nucl. Phys. A*, 804, 309, doi: [10.1016/j.nuclphysa.2008.01.005](https://doi.org/10.1016/j.nuclphysa.2008.01.005)
- Serot, B. D., & Walecka, J. D. 1986, *Adv. Nucl. Phys.*, 16, 1

- Takahashi, H., et al. 2001, *Phys. Rev. Lett.*, 87, 212502, doi: [10.1103/PhysRevLett.87.212502](https://doi.org/10.1103/PhysRevLett.87.212502)
- Tews, I., Lattimer, J. M., Ohnishi, A., & Kolomeitsev, E. E. 2017, *Astrophys. J.*, 848, 105, doi: [10.3847/1538-4357/aa8db9](https://doi.org/10.3847/1538-4357/aa8db9)
- Tews, I., Margueron, J., & Reddy, S. 2018, *Phys. Rev. C*, 98, 045804, doi: [10.1103/PhysRevC.98.045804](https://doi.org/10.1103/PhysRevC.98.045804)
- . 2019, *Eur. Phys. J. A*, 55, 97, doi: [10.1140/epja/i2019-12774-6](https://doi.org/10.1140/epja/i2019-12774-6)
- Todd-Rutel, B., & Piekarewicz, J. 2005a, *Phys. Rev. Lett.*, 95, 122501, doi: [10.1103/PhysRevLett.95.122501](https://doi.org/10.1103/PhysRevLett.95.122501)
- Todd-Rutel, B. G., & Piekarewicz, J. 2005b, *Phys. Rev. Lett.*, 95, 122501, doi: [10.1103/PhysRevLett.95.122501](https://doi.org/10.1103/PhysRevLett.95.122501)
- Tolman, R. C. 1934, *Proc. Nat. Acad. Sci.*, 20, 169, doi: [10.1073/pnas.20.3.169](https://doi.org/10.1073/pnas.20.3.169)
- Tsang, M., et al. 2012, *Phys. Rev. C*, 86, 015803, doi: [10.1103/PhysRevC.86.015803](https://doi.org/10.1103/PhysRevC.86.015803)
- Walecka, J. 1974, *Annals Phys.*, 83, 491, doi: [10.1016/0003-4916\(74\)90208-5](https://doi.org/10.1016/0003-4916(74)90208-5)
- Wei, J., Figura, A., Burgio, G., Chen, H., & Schulze, H. 2019, *J. Phys. G*, 46, 034001, doi: [10.1088/1361-6471/aaf95c](https://doi.org/10.1088/1361-6471/aaf95c)
- Weissenborn, S., Chatterjee, D., & Schaffner-Bielich, J. 2012, *Phys. Rev.*, C85, 065802, doi: [10.1103/PhysRevC.85.065802](https://doi.org/10.1103/PhysRevC.85.065802); [10.1103/PhysRevC.90.019904](https://doi.org/10.1103/PhysRevC.90.019904)
- Xie, W.-J., & Li, B.-A. 2019, *Astrophys. J.*, 883, 174, doi: [10.3847/1538-4357/ab3f37](https://doi.org/10.3847/1538-4357/ab3f37)
- Yang, F., & Shen, H. 2008, *Phys. Rev. C*, 77, 025801, doi: [10.1103/PhysRevC.77.025801](https://doi.org/10.1103/PhysRevC.77.025801)
- Zhang, N.-B., & Li, B.-A. 2019, *J. Phys. G*, 46, 014002, doi: [10.1088/1361-6471/aaef54](https://doi.org/10.1088/1361-6471/aaef54)
- Zhang, N.-B., Li, B.-A., & Xu, J. 2018, *Astrophys. J.*, 859, 90, doi: [10.3847/1538-4357/aac027](https://doi.org/10.3847/1538-4357/aac027)
- Zhao, T., & Lattimer, J. M. 2018, *Phys. Rev. D*, 98, 063020, doi: [10.1103/PhysRevD.98.063020](https://doi.org/10.1103/PhysRevD.98.063020)
- Zhou, E.-P., Zhou, X., & Li, A. 2018, *Phys. Rev. D*, 97, 083015, doi: [10.1103/PhysRevD.97.083015](https://doi.org/10.1103/PhysRevD.97.083015)
- Zhu, Z.-Y., Zhou, E.-P., & Li, A. 2018, *Astrophys. J.*, 862, 98, doi: [10.3847/1538-4357/aacc28](https://doi.org/10.3847/1538-4357/aacc28)